A calculation of cricket ball trajectories

C J Baker
School of Civil Engineering, University of Birmingham, Edgbaston, Birmingham B15 2TT, UK
email: C.J.Baker@bham.ac.uk

The manuscript was received on 12 September 2009 was accepted after received for publication on 23 November 2009.

DOI: 10.1243/09544062JMES1973

Abstract: While a number of past investigations have measured the aerodynamic forces on cricket balls, in general these forces have not been used to calculate the trajectories of balls between bowler and batsman. This article presents such a calculation. It begins with the full trajectory equations as developed for the study of debris flight in extreme windstorms, which are adapted for the cricket ball case. A collation of earlier experimental data is then presented for drag and side force coefficients on cricket balls. From these data, which show considerable scatter, a small number of generic force characteristics are derived for use in the trajectory equations. These characteristics have constant force coefficients in the subcritical and supercritical Reynolds number regions, and a transition between these two regions with a variable gradient. An approximate analysis of the trajectory equations results in very simple forms for the trajectories in the sub- and supercritical Reynolds number regimes, which reveal the governing dimensionless parameters of the problem, and enable the effect of crosswinds to be quantified. The predicted parabolic profiles are in agreement with some very simple calculations carried out by earlier investigators, revealing the limited range of validity of such calculations, and with the limited real bowling trajectories that have been observed. A full solution of the trajectory equations is then presented for the generic force coefficient characteristics, and a study of trajectories through the Reynolds number range is carried out. In the transition region between sub- and supercritical flows, complex ball trajectories are shown to be possible.

Keywords: sports ball aerodynamics, trajectory modelling, cricket, bowling

1 INTRODUCTION

One of the most important facets of fast bowling in cricket is the ability of bowlers to make the ball 'swing' or deviate laterally from its course between leaving the bowler's hand and arriving at the position of the batsman. Experience suggests that this is associated with the way in which the ball is bowled and in particular with the position of the 'seam' relative to the bowling direction. This seam holds the outer surfaces of the two sides of the ball together and the stitches of the seam protrude above the surface of the ball. Swing bowlers will bowl the ball with the seam in a vertical plane inclined at an angle to the bowling direction. The roughness of the ball is also known to be of importance, and bowlers will polish one side of the ball (the side that is 'leading' the seam through the air) to help achieve swing. Over the last few decades a number of investigators have carried out experiments on cricket balls to understand this phenomenon, mainly through force measurements on stationary balls, with and without spin, in wind tunnels of different types. Much of this work is reviewed in the work of Mehta [**1**–**3**]. These experiments have determined the drag and side forces on cricket balls under a variety of conditions, and have elucidated the primary mechanisms of the different types of swing behaviour that have been observed. However, most of these investigations lack context, in that the measured forces are not related to actual swing trajectories that are, of course, of primary importance to both batsman and bowler. The exception to this is the work of Bentley *et al.* [**4**], which reports trajectory measurements made with certain major simplifications, and will be discussed further below. This article addresses this issue and studies the trajectories of cricket balls with different types of aerodynamic force profile. This work is based on the recent work by the author in predicting

the trajectories of flying debris during extreme windstorms [**5**] and predicting the flight of ballast beneath high-speed trains [**6**].

In section 2 the trajectory equations are outlined and expressed in a dimensionless form that reveals the fundamental parameters of the problem. Section 3 reviews the various investigations that have been carried out in the past, collates the aerodynamic force coefficients that have been measured, and discusses the explanations that have been offered in the past for the swing phenomenon. The results of these investigations are then used to derive a set of generic force characteristics for further study. Section 4 then sets out an approximate analysis of the trajectory equations, which results in some very simple equations for swing under specific conditions, which, through a comparison with the full solutions of the trajectory equations, are shown to be surprisingly accurate. These give a useful physical insight into the issues involved and reveal the broad effect of crosswind on cricket ball swing. Section 5 then presents a full solution of the trajectory equations for more general conditions and discusses more complex phenomena such as lateswing and reverse swing. Some concluding remarks are made in section 6.

2 TRAJECTORY EQUATIONS

Baker [**5**] sets out equations for the flight of both compact debris (with the three length dimensions broadly comparable with each other) and sheet debris (with two major and one minor length dimension) under extreme wind conditions, such debris having recently been recognized as one of the major causes of building damage in severe windstorms. These winds accelerate the debris from zero velocity to velocities close to the wind velocity. In Quinn *et al.* [**6**], the authors utilize the compact debris equations further to investigate the flight of ballast under high-speed trains, an issue that is becoming to be of increasing concern for high-speed train operators. This involved the specification of the air velocity underneath the trains. Again the air movements under the train accelerate the ballast from stationary to velocities close to the train-induced air velocities. In studying cricket ball trajectories it is appropriate to again use the compact debris equations, but with the difference that this time the object under consideration is moving much faster than the prevailing air velocities due to natural wind. Applying Newton's Law in the x (along the pitch), y (across the pitch), and z (vertical) directions and suitably non-dimensionalizing, one obtains the basic trajectory equations for cricket balls

$$\frac{\mathrm{d}\bar{u}}{\mathrm{d}t} = -\left[(\bar{u}-\bar{U})^2 + (\bar{v}-\bar{V})^2 + (\bar{w}-\bar{W})^2\right]^{0.5} \times (\bar{u}-\bar{U})C_{\mathrm{D}}T \tag{1}$$

$$\frac{\mathrm{d}\bar{v}}{\mathrm{d}t} = -\left[(\bar{u}-\bar{U})^2 + (\bar{v}-\bar{V})^2 + (\bar{w}-\bar{W})^2\right]^{0.5} \times \left[-C_{\mathrm{D}}T(\bar{v}-\bar{V}) + C_S T(\bar{u}-\bar{U})\right] \tag{2}$$

$$\frac{\mathrm{d}\bar{w}}{\mathrm{d}t} = -\left[(\bar{u}-\bar{U})^2 + (\bar{v}-\bar{V})^2 + (\bar{w}-\bar{W})^2\right]^{0.5} \times (\bar{w}-\bar{W})C_{\mathrm{D}}T - 1 \tag{3}$$

Here $\bar{u}$, $\bar{v}$, and $\bar{w}$ are the cricket ball velocities in the x-, y-, and z-directions, respectively, non-dimensionalized by dividing by the initial speed at which the ball is bowled, q. $\bar{t}$ is the non-dimensional time from the release of the ball tg/q. $\bar{U}$, $\bar{V}$, and $\bar{W}$ are the wind velocities in the x, y, and z directions, respectively, again normalized with q. C_{D} and C_{S} are the aerodynamic drag and side coefficients defined as

$$C_{\mathrm{D}} = \frac{D}{0.5\rho A Q^2} \tag{4}$$

$$C_{\mathrm{S}} = \frac{S}{0.5\rho A Q^2} \tag{5}$$

where D and S are the drag and side forces, respectively, A is the ball cross-sectional area, ρ is the density of air, and Q is the total relative velocity of the ball relative to the air $[(\bar{u}-\bar{U})^2 + (\bar{v}-\bar{V})^2 + (\bar{w}-\bar{W})^2]^{0.5}$. T is the Tachikawa number [**7**] given by

$$T = \frac{\rho A q^2}{2\,\mathrm{mg}} \tag{6}$$

where m is the mass of the ball. This represents the ratio of the initial flow inertia force on the ball to the

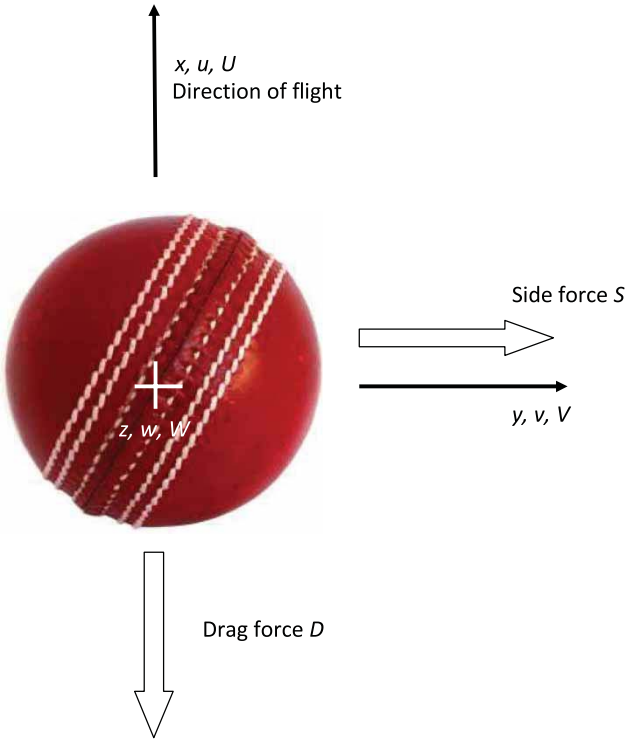

Fig. 1 Axis system, velocities, and forces

weight of the ball. It can thus be seen from equations (1) to (3) that the governing parameters of the problem are the product side and drag force coefficients and the Tachikawa number. The axis system and the aerodynamic forces are illustrated in Fig. 1.

3 DRAG AND SIDE FORCE COEFFICIENTS

To solve the trajectory equations (1) to (3), a knowledge of the drag and side force coefficients is required. These parameters have been measured by a number of researchers in the past using a variety of experimental techniques. Experiments have been carried out on real cricket balls and model cricket balls of various scales, for different seam angles, with and without spin around the seams. These are fully discussed in the papers by Mehta in references [**1**] to [**3**]. In this section a compilation of these results is made, although it must be acknowledged that doubts exist concerning the adequacy of some of the experimental techniques that have been used. This compilation is then used to derive a small number of generic force coefficient characteristics that will be used in trajectory calculations in what follows.

It is to be expected that the basic parameter on which the drag and side force coefficients depends will be the ball Reynolds number $Re = q\rho d/\mu$, where d is the diameter of the cricket ball and μ is the dynamic viscosity of air. Thus in what follows, all the available data will be plotted against this parameter. In the compilation, data will be used from the following sources.

1. Alam *et al.* [**8**, **9**] give the same extensive results for cricket ball drag for a number of different ball types, with different seam orientations (denoted by A-max and A-min for the maximum and minimum values at a particular Reynolds number).
2. Barton [**10**] describes measurements with cricket balls mounted on a pendulum, for both old and new cricket balls (denoted Ba-n, where n is the seam angle to the effective direction of flight). He also carried out experiments where the ball trajectory was measured for different seam configurations, after rolling down a ramp to create spin into the wind tunnel flow, where the side force was measured indirectly through trajectory measurements. There was, however, very considerable scatter in the results that were obtained and will not be considered further in this article.
3. Bentley *et al.* [**4**] describe experiments where the forces on the cricket ball were again calculated from measured trajectories after the ball was rolled into the tunnel, as in the experiments of Barton, for different seam configurations and spin rates (denoted by B-n-m revolution/s, where n is the seam angle and m is the spin rate in revolutions per second).
4. Hunt [**11**] and Ward [**12**], both presented in reference [**1**], describe undergraduate project work on a large-scale model cricket ball, where forces were measured using a strain gauge balance (denoted by H-n and W-n).
5. Sayers [**13**] describes extensive wind tunnel experiments carried out on large models of cricket balls with different roughness configurations (S-n).
6. Sayers and Hill [**14**] describe wind tunnel measurements of the forces on real cricket balls of various types (SH-n).
7. Sherwin and Sproston [**15**] give forces for real cricket balls measured using a force balance within a wind tunnel (Sh-n).

Figure 2 shows data for the variation of drag coefficient with Reynolds number for both new and old cricket balls for a variety of seam angles (or for models of cricket balls of various types). The new balls have a high degree of polish on either side of the seam, while the old balls are polished on the one side of the seam and worn and rough on the other. It can be seen that for all the results shown, there is a broad consistency, with the drag coefficient tending to values of around 0.5 for higher Reynolds numbers. Note, however, that all the experiments are for essentially subcritical flows (i.e. the Reynolds number is not high

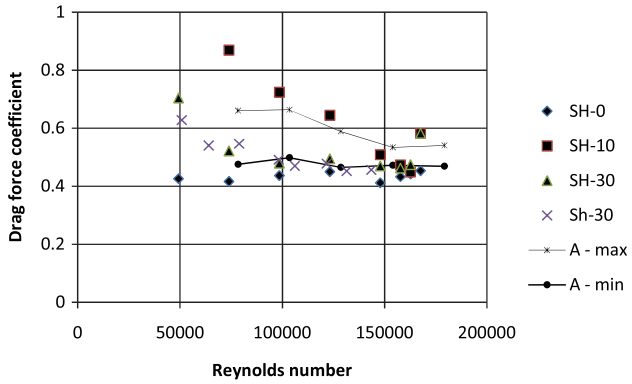

(a) Smooth sphere / new ball

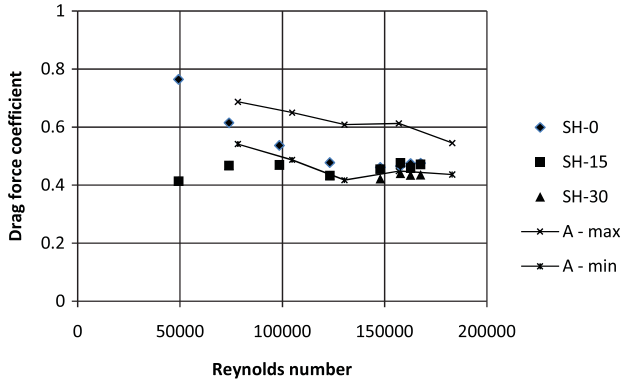

(b) Rough sphere / old ball

Fig. 2 Compilation of cricket ball drag coefficient data

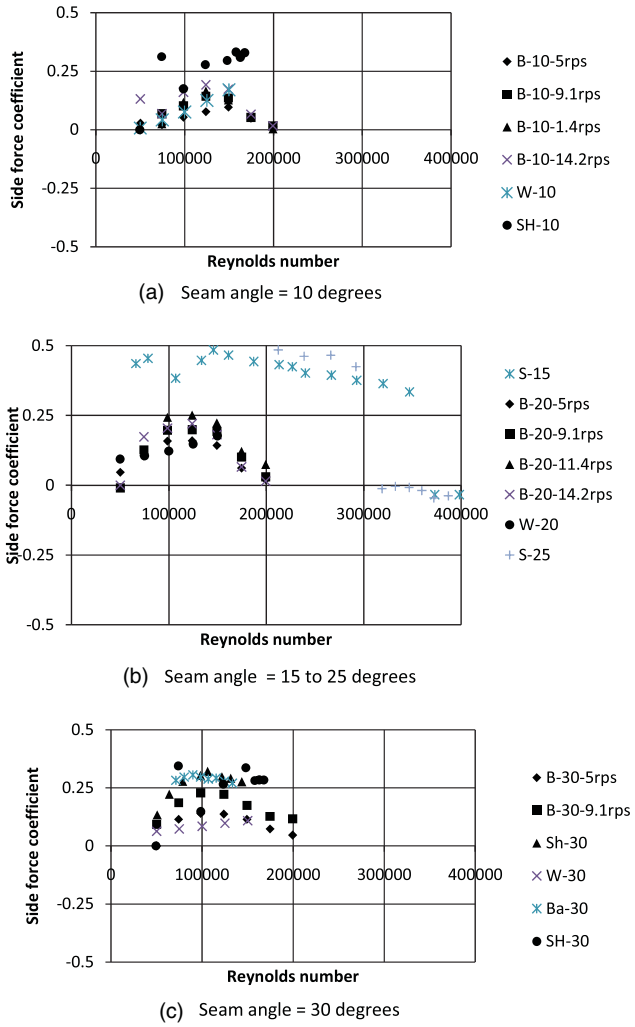

Fig. 3 Compilation of side force coefficient data for smooth spheres/new balls

enough to establish a fully turbulent wake). At higher Reynolds numbers one would expect a 'drag crisis' in which the drag falls to around 0.3 over a small range of Reynolds numbers.

Figure 3 shows data for the side force coefficient for new balls for a variety of seam angle ranges. It can be seen that there is very considerable scatter between the results. In general, however, the side force coefficient increases from zero at a Reynolds number of around 0.25–0.5 $\times$ 10^5, plateaus at values of around 1.0 $\times$ 10^5, and then falls off at higher Reynolds numbers. The general explanation offered for this is that the presence of the seam causes the boundary layer on the ball surface to become turbulent on the seam side of the ball, while the boundary layer remains laminar on the non-seam side of the ball. This results in different separation positions on either side of the seam (with the turbulent seam side boundary layer separating further around the ball), and thus an asymmetric wake and a consequent side force, resulting in the observed swing of the ball in flight. At higher Reynolds numbers the fall in side force coefficient reflects the fact that the boundary layer on the non-seam side of the ball becomes turbulent and separates further around the ball, thus making the wake more symmetric. This is most clearly seen in the experiments in reference [**14**], although the fall in side force coefficient occurs at an anomalously high Reynolds number in this case, presumably because the large-scale model that was used in these experiments was unrepresentatively smooth. At higher Reynolds numbers the force coefficients are close to zero. It would also be expected that the drag coefficient would also decrease in this Reynolds number range (the drag crisis referred to above), although the experimental Reynolds numbers in Fig. 1 are not high enough to reflect this. It is further to be expected that the values of side force coefficient with Reynolds number will depend on the angle of inclination of the seam to the flow and also on the spin rate of the balls. However, specific trends are hard to discern from the experimental results, although the results tend to indicate an optimum seam angle of around 20° (i.e. for maximum side force coefficient) and the results of reference [**4**] suggest an increase in the side force coefficient with spin rate.

Figure 4 shows a similar compilation of results for old balls (i.e. with the ball polished on the one side of the seam and worn on the other side). At subcritical Reynolds numbers the behaviour is similar, but with large variations in absolute values of the coefficient. At higher Reynolds numbers, there is an indication that the side force coefficient can take on negative values, which results in so-called 'reverse swing' (i.e. in the opposite direction to that expected at lower Reynolds numbers). In these conditions the boundary layer will be turbulent on both sides of the ball, and might be expected to separate symmetrically. Mehta [**1–3**] hypothesizes that the negative side forces are due to the fact that the turbulent boundary layer is thicker on the seam side of the ball, due to the disturbance caused by the seam, and thus more prone to separate earlier than the turbulent boundary layer on the non-seam side of the ball. This will again result in an asymmetric wake, but in an opposite sense to that described above, with a consequent negative side force.

From the above results, scattered as they are, a number of points are clear.

1. It is possible to identify subcritical and supercritical Reynolds numbers regimes in which the side and drag force coefficients are broadly constant, although the absolute magnitudes of these coefficients vary from test to test.
2. Between these two regimes there is a transition of some sort, which may be quite steep in Reynolds number terms (over, say, 0.1 $\times$ 10^5) or more shallow (over 0.4 $\times$ 10^5 or more).

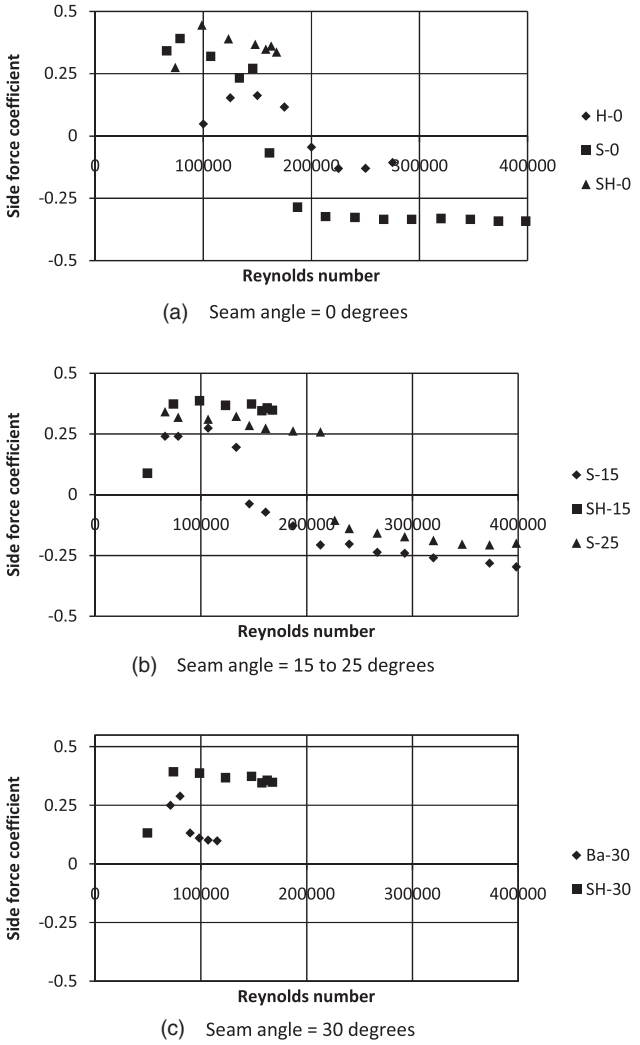

Fig. 4 Compilation of side force coefficient data for semi-roughened spheres/old balls

3. The effect of spin rate on the force coefficients is not clear.

Now the standard explanations of the side force variation with Reynolds number, based on boundary layer separation positions, seem to be plausible. However, the author would ask whether these explanations are a little too simplistic: they implicitly relate the flow around a three-dimensional (3D) sphere to that around a 2D cylinder in terms of boundary layer behaviour, although it is by no means clear that the boundary layer would behave in precisely the same way. Also the effects of spin are largely ignored in the explanations of the aerodynamic force variation, although there is recent evidence that this may significantly affect the flow around the ball [**16**]. Spin can be expected to affect the boundary layer development through an increase in the effective flow velocity on the top of the ball and a decrease in the effective flow velocity on the bottom of the ball, and may also result in cellular secondary flows over the ball surface. The assumed nature of the transition from the sub- to the supercritical flow regime is also implicitly considered as gradual, with a well-defined fall in the coefficients through the transition region. However, experience would suggest that in this region the flow is very unstable, with rapid changes from the subcritical to the supercritical force coefficients with small changes in Reynolds number. The average values shown in Figs 3 and 4 may well represent a rather artificial average of two intermittent flow regimes. Also, hysteresis effects in the wind tunnel experiments could be expected to be of importance, with subcritical conditions being sustained to higher Reynolds numbers as wind tunnel speed is increased, and supercritical conditions being sustained to lower Reynolds number as wind speed is decreased. A complete and more nuanced explanation of the causes of swing will require much more detailed observations of the boundary layer development around a spinning ball.

This point being made however, in some sense the cause of cricket ball side and drag force is not relevant to the main thrust of this article: the calculation of cricket ball trajectories. It is sufficient to quantify the measured drag and side force coefficients, with or without an adequate explanation of their variation with Reynolds number. In what follows four idealized generic forms are adopted for these coefficients as follows (Fig. 5). In all these forms the increase in the side force coefficient at low Reynolds numbers is neglected, as this will occur at low bowling speeds (<50 mile/h) that will not be considered in what follows. The side

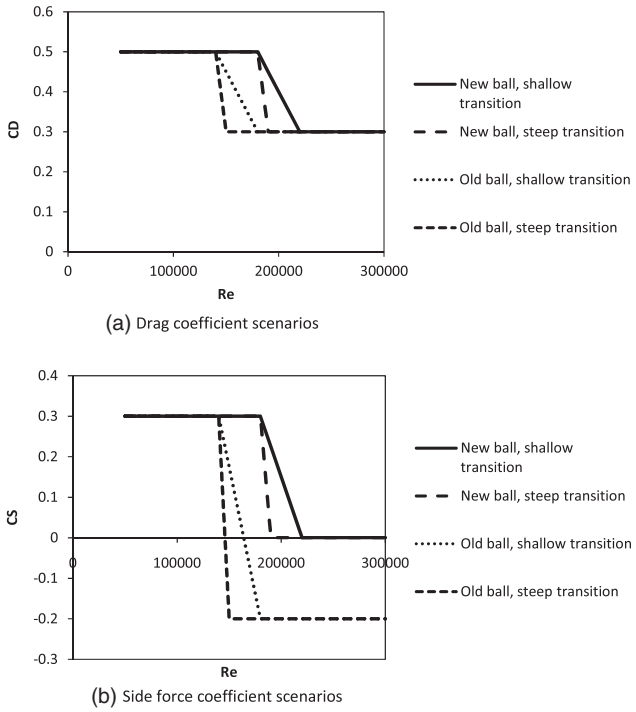

Fig. 5 Force coefficient scenarios for trajectory calculations

and drag force coefficients are then assumed constant in the subcritical range up to a transition Reynolds number. The side and drag coefficients then decrease through this transition to another constant value in the supercritical range. Based on a broad consideration of the data presented in Figs 2 to 4, the four generic forms are as follows.

1. New ball, shallow transition. Subcritical drag and side force coefficients of 0.5 and 0.3, respectively, and supercritical coefficients of 0.3 and 0, respectively. The transition begins at a Reynolds number of 1.8×10^5 (corresponding to a bowling speed of 81 mile/h) and is complete by a Reynolds number of 2.2×10^5 (100 mile/h).
2. New ball, steep transition. As above, but with the transition ending at a Reynolds number of 1.9×10^5 (86 mile/h).
3. Old ball, shallow transition. The subcritical coefficient drag and side force coefficient values are 0.5 and 0.3, respectively, as for the new ball, but with supercritical values of 0.3 and −0.2, respectively. The transition begins at a Reynolds number of 1.4×10^5 (63 mile/h) and ends at a Reynolds number of 1.8×10^5 (81 mile/h).
4. Old ball, steep transition. As above, but with the transition ending at a Reynolds number of 1.5×10^5 (68 mile/h).

4 APPROXIMATE SOLUTIONS

4.1 No-wind case

In this section an approximate solution to the trajectory equations for the no-wind condition (i.e. $\bar{U} = \bar{V} = \bar{W} = 0$) and also for the case where the drag and the side force coefficients are constant (i.e. on the sub- and supercritical branches of the generic force coefficient distributions) of Fig. 5 is considered. Assume that the lateral and vertical ball velocities are much smaller than the longitudinal velocities. In this case the trajectory equations reduce to

$$\frac{\mathrm{d}\bar{u}}{\mathrm{d}t} = -C_\mathrm{D} T \bar{u}^2 \tag{7}$$

$$\frac{\mathrm{d}\bar{v}}{\mathrm{d}t} = -C_\mathrm{S} T \bar{u}^2 \tag{8}$$

$$\frac{\mathrm{d}\bar{w}}{\mathrm{d}t} = -1 \tag{9}$$

These are easily integrable analytically and result in the following expressions for the dimensionless ball velocities and displacements in terms of dimensionless time

$$\bar{u} = \frac{1}{1 + C_\mathrm{D} T \bar{t}} \tag{10}$$

$$\bar{v} = \left(1 - \frac{1}{1 + C_\mathrm{D} T \bar{t}}\right) \frac{C_\mathrm{S}}{C_\mathrm{D}} \tag{11}$$

$$\bar{w} = \sin\alpha - \bar{t} \tag{12}$$

$$\bar{x} = \frac{1}{C_\mathrm{D} T} \log(1 + C_\mathrm{D} T \bar{t}) \tag{13}$$

$$\bar{y} = \left(\bar{t} - \frac{1}{C_\mathrm{D} T} \log(1 + C_\mathrm{D} T \bar{t})\right) \frac{C_\mathrm{S}}{C_\mathrm{D}} \tag{14}$$

$$\bar{z} = \bar{t} \sin\alpha - \frac{\bar{t}^2}{2} \tag{15}$$

Here α is the initial angle of inclination in the x–z plane (i.e. the angle to the vertical at which the ball is bowled). Note that the lateral and vertical trajectories are effectively independent of each other, with only the latter being a function of the initial angle α. Now, eliminating the dimensionless time between the longitudinal and lateral displacement equations (13) and (14) gives the following expression for the lateral trajectory

$$\bar{y} = \frac{C_\mathrm{S}}{C_\mathrm{D}^2 T^2} (e^{C_\mathrm{D} T \bar{x}} - 1 - C_\mathrm{D} T \bar{x}) \tag{16}$$

Now the product $C_\mathrm{D} T \bar{x}$ can be shown to be of the order of 0.1 to 0.2 and thus equation (16) approximates to

$$\bar{y} = \frac{C_\mathrm{S} T}{2} \bar{x}^2 \tag{17}$$

Figure 6(a) shows a comparison between the displacement predicted using equation (17) and those predicted from a full solution of equations (1) to (3) for the new ball, subcritical *Re* case for a range of bowling speeds. The ball mass is taken as 0.16 kg, and the ball diameter as 0.072 m. The lateral displacements are given at a distance of 18 m from the bowling position – roughly corresponding to the position of the batsman. Agreement can be seen to be good, with differences between the approaches of the order of a few millimetres (note the large y-axis scales), and a close examination of the results confirms the approximations made above concerning the smallness of the lateral and vertical velocities and the product $C_\mathrm{D} T \bar{x}$. It can thus be seen that, as a good approximation, the dimensionless trajectory is parabolic, with the constant of proportionality being the product of the side force coefficient and the Tachikawa number. From the definitions of these parameters given in equations (4) to (6), this can be seen to be proportional to the ratio of the side force to the weight of the cricket ball – the so-called 'swing force ratio' of reference [**13**], also used in the presentation of results in the various works of Mehta. Perhaps more remarkably, if one substitutes the definitions of Tachikawa number from equation (6) and expresses the distances in dimensional terms, equation (17) becomes

$$y = \frac{C_\mathrm{s} \rho A}{4\,m} x^2 \tag{18}$$

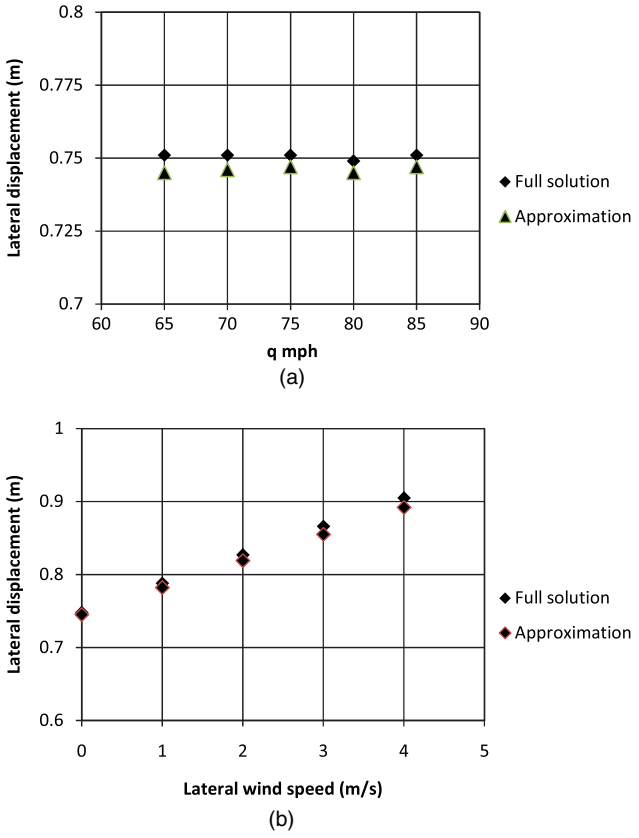

Fig. 6 Accuracy of approximate methods

and thus the trajectory is independent of the initial speed (although the time it takes to follow that trajectory varies with throwing speed). Substituting the values for density of air, cricket ball mass, and area, one obtains

$$y = 0.0077 C_S x^2 \tag{19}$$

and assuming a side force coefficient of 0.3, this gives a swing of 0.75 m at $x = 18$ m. Thus, under the specific conditions that apply to this approximation with the flow conditions always in a region of constant side force coefficient, the amount of swing is directly proportional to the value of this coefficient.

In a similar way one may write the following formulae for the longitudinal and lateral velocities in terms of dimensionless distance

$$\bar{u} = e^{-C_D T \bar{x}} \tag{20}$$

$$\bar{v} = (1 - e^{-C_D T \bar{x}}) \frac{C_S}{C_D} \tag{21}$$

Again, assuming that is $C_D T \bar{x}$ small, one obtains

$$\bar{u} = 1 - C_D T \bar{x} \tag{22}$$

$$\bar{v} = C_S T \bar{x} \tag{23}$$

which in dimensional terms are

$$u = \left(1 - \frac{C_D \rho A}{2m} x\right) q \tag{24}$$

$$v = \left(\frac{C_s \rho A}{2m} x\right) q \tag{25}$$

Substituting the values for density of air, cricket ball mass, and area, one obtains

$$u = (1 - 0.0155 C_D x) q \tag{26}$$

$$v = (0.0155 C_s x) q \tag{27}$$

For a value of x of 18 m, and drag and side force coefficients of 0.5 and 0.3, respectively, this gives $u = 0.860q$ and $v = 0.084q$. Thus at the batsman's position the ball velocity will be 86 per cent of the bowling velocity in the longitudinal direction and 8 per cent of the bowling velocity in the transverse direction for the assumptions made. The first figure is rather less than that has been assumed by some authors in the past [**1**, **10**].

Now Bentley *et al.* [**4**] also calculated ball trajectories by making the simple assumption that the side force on the ball is constant and that the speed of the ball along the pitch does not vary. Clearly, neither of these assumptions are completely valid as the velocity will fall by around 14 per cent and thus, for constant force coefficients, the side force will fall by around twice that. Nonetheless the application of these assumptions to the trajectory equations results in an expression for the lateral trajectory that is identical with equation (18), although the precise position of the ball along the trajectory at any one time is very different, because the speed of the ball is not allowed to vary. The analysis in this article does, however, specify limits to the validity of the simple assumptions, showing that they are only adequate for the trajectory under conditions of constant force coefficient, and that these assumptions cannot give an accurate position of the ball along the trajectory at a specific time. Mehta [**1**] also notes that the predicted trajectories at high bowling speeds are very similar: the same conclusion as noted above. Finally, it should be noted that Imbrosciano [**17**] presents measured cricket ball trajectories that do indeed have a parabolic shape, thus confirming both the work of reference [**4**] and the current analysis.

4.2 Crosswind case

Now consider a similar approach for the case of a small crosswind (i.e. $\bar{U} = \bar{W} = 0$, and $\bar{V}_- \ll \bar{u}$). In this case the longitudinal and vertical equations of motion remain the same as equations (7) and (9), but the lateral displacement equation becomes

$$\frac{\mathrm{d}\bar{v}}{\mathrm{d}\bar{t}} = C_D T \bar{u} \bar{V} + C_s T \bar{u}^2 \tag{28}$$

The solution to equation (28) is again quite straightforward, and results in the following approximation for the dimensionless trajectory

$$\bar{y} = \frac{(C_S + C_D \bar{V})T}{2} \bar{x}^2 \tag{29}$$

This is of the same form as equation (18) and reveals that the effect of a crosswind is to increase the constant of proportionality in the parabolic trajectory equation. Figure 6(b) shows a comparison of the results of equation (20) with predicted trajectory values from equations (1) to (3) for a bowling speed of 75 mile/h and a range of wind speeds. Again the agreement can be seen to be excellent. Note that the average hourly wind speed 10 m above the ground level in England is of the order of 4 m/s [**18**]. The variation of this velocity with height is approximately logarithmic and for a ground roughness typical of cricket pitches (around 0.01 m), it can be shown that this velocity corresponds to a velocity of 2.7 m/s at 1.0 m above the ground: the approximate average height of a cricket ball trajectory. At this speed, the average deflection due to wind effects alone is of the order of 10 cm.

5 FULL SOLUTIONS OF TRAJECTORY EQUATIONS

5.1 New ball

Figure 7 shows the lateral and vertical trajectory calculations for the new ball, shallow transition force coefficient characteristic. The initial inclination angle α is chosen for each velocity such that the ball falls a height of 2.5 m after a longitudinal distance of 18 m, corresponding to a fully pitched delivery. This angle varied between -0.064 and -0.091 radians as the bowling speed increased. It can be seen that as the bowling speed increases from 80 to 100 mile/h, the value of swing falls. At higher (and unrealistic) bowling speeds, the value of swing approaches zero as the side force coefficient falls to zero. The reduction in swing is gradual, however. There is little variation in the vertical trajectories through the speed range. Figure 8 shows similar figures for the steep transition case, with values of the initial inclination angle varying between -0.067 and -0.088 radians as the speed increases. Here the speed range over which the swing falls to zero is much narrower: from 80 to 90 mile/h. In both cases the lower wind speed shown (at 80 mile/h) corresponds to the completely subcritical case and is well approximated by equation (18). The importance of the transition Reynolds number and the slope of the transition in determining the swing trajectory of the ball are clear. Again there is little variation in the vertical profile. Figure 9 illustrates the steep transition case further, showing the variation of the normalized longitudinal and lateral velocities distance along the pitch. At lower bowling speeds, the ball is in the subcritical regime with high drag (and thus a large fall off in longitudinal velocity along the pitch) and high side force coefficient (and thus large lateral velocities). At higher bowling speeds, the ball

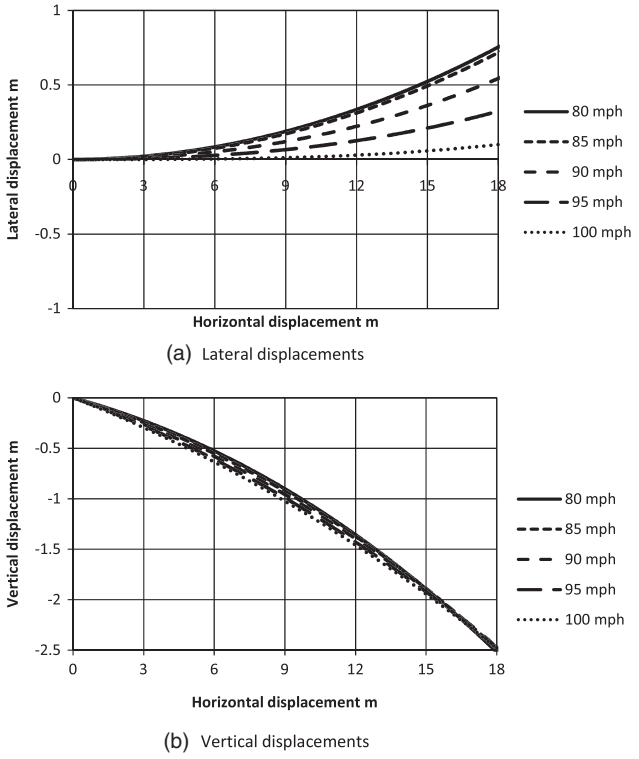

Fig. 7 Trajectories for new ball/shallow transition scenario

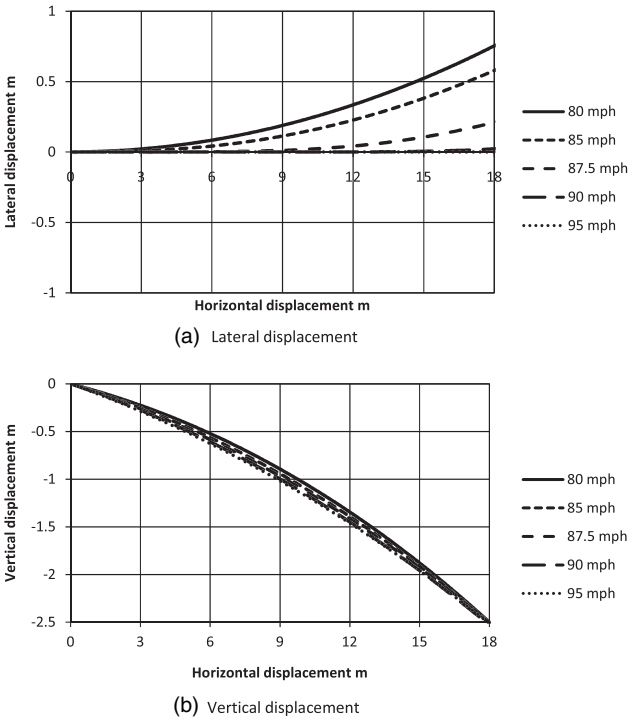

Fig. 8 Trajectories for new ball/steep transition scenario

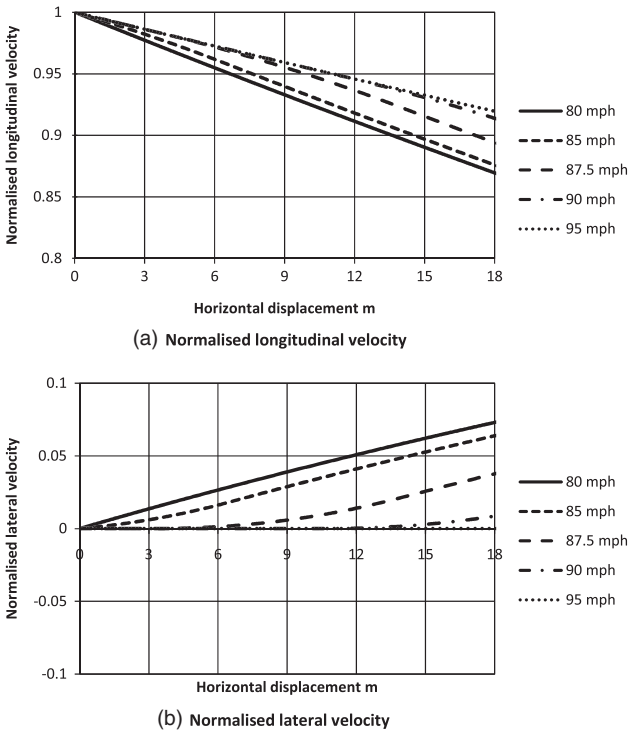

Fig. 9 Normalized longitudinal and lateral velocities for new ball/steep transition scenario

is in the supercritical region, with lower drag coefficient, and thus a smaller fall in longitudinal velocity, and zero side force coefficient, and thus zero lateral velocity.

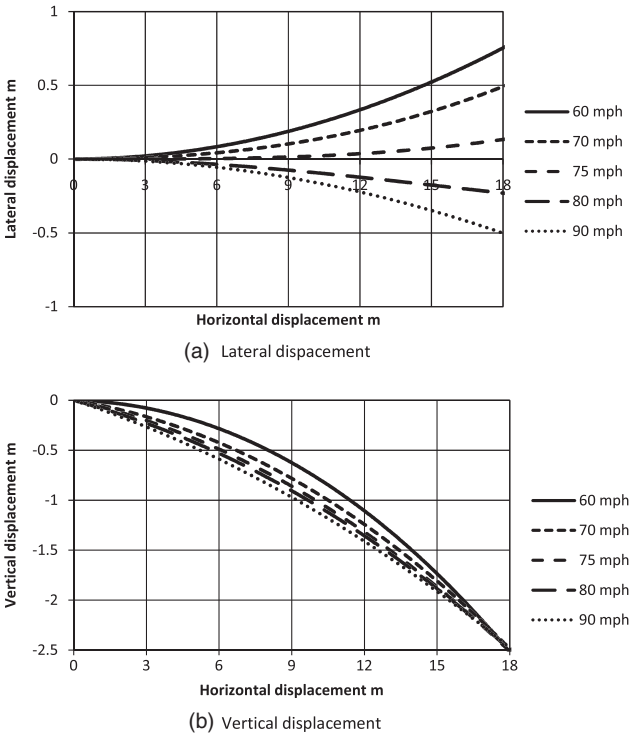

Fig. 10 Trajectories for old ball/shallow transition scenario

5.2 Old ball

Figure 10 shows the old ball, shallow transition calculations. Again the initial inclination angle was chosen to give a fall of 2.5 m after 18 m and varied between −0.005 and −0.04 radians as the bowling speed increased. As the speed increases from 60 to 90 mile/h, the swing moves from positive to negative. Again the 60 mile/h case is well approximated by equation (18). Of particular interest is the 75 mile/h case, where there is little movement for the first half of the trajectory, followed by a movement of about 0.1 m over the last half. In this case the vertical trajectories show some variation with wind speed. Figure 11(a) shows the results for the steep trajectory case. Here, only a very narrow range of bowling speeds is shown (from 64 to 72 mile/h) and it can be seen that is a very rapid change in the trajectory as the speed increases. The

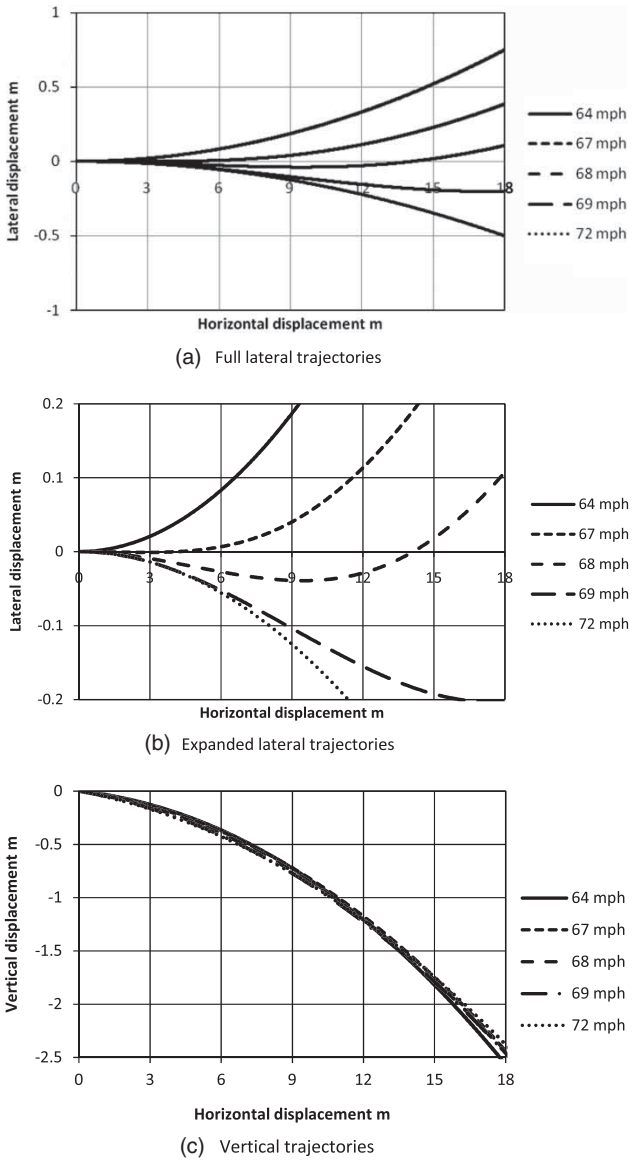

Fig. 11 Trajectories for old ball/steep transition scenario

initial inclination angle is between −0.024 and −0.042 radians. As the bowling speed increases from 67 to 69 mile/h, the trajectory changes very markedly from positive to negative swing. The situation at 68 mile/h is particularly complex and shows both positive and negative displacements. This is better illustrated in the expanded version of Fig. 11(b). The vertical trajectories in Fig. 11(c) show little variation. Again further insight can be obtained by a study of the non-dimensional longitudinal and lateral velocity variation shown in Fig. 12. The fall in longitudinal velocity along the pitch reduces as bowling speed increases, and drag coefficient decreases through the transition. The lateral velocity goes from positive to negative as the bowling speed passes through the transition, as the side force coefficient goes from positive to negative. The complex patterns are due to a fall in the bowling speed along the pitch, which results in high velocities and negative side forces just after the ball is bowled (i.e. the ball is towards the supercritical end of the transition) and lower velocities (due to the reduction in longitudinal velocity) and positive side forces closer to the batsman. Note again that the upper and lower curves at 64 and 72 mile/h are again well approximated by the simple expressions given in the last section. Mehta [**1**] suggests that the observed phenomenon of late swing is in reality simply due to the parabolic path of the ball, where the magnitude of the lateral displacement increases markedly with distance from the bowler, and thus the batsman would perceive more swing to occur as the ball approaches. The analysis presented here would however suggest that late swing is a real phenomenon, but only possible in a narrow Reynolds number range for specific ball conditions.

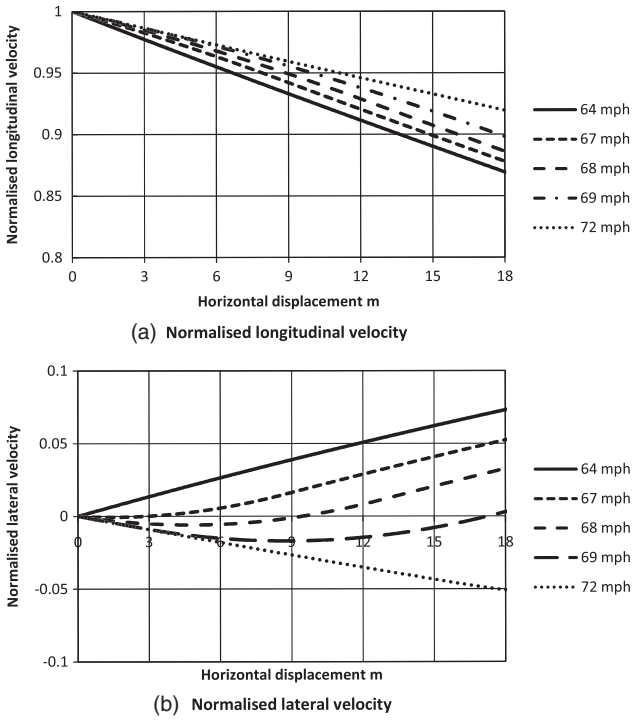

Fig. 12 Normalized longitudinal and lateral velocities for new ball/steep transition scenario

6 CONCLUSIONS AND SUGGESTIONS FOR FUTURE WORK

From the above analysis the following conclusions can be drawn.

1. Trajectory equations show that the governing dimensionless groups that describe the flight of cricket balls are the products of the Tachikawa number with the drag and side force coefficients.
2. A collation of experimental data shows considerable scatter, but does clearly show that cricket balls display sub- and supercritical Reynolds number regimes, in which the drag and side forces are reasonably constant, with a transition region of variable force coefficient gradient.
3. The supercritical values of the side force coefficient are in general zero for new balls, and less than zero for old balls.
4. An approximate analysis of the trajectory equations shows that, for constant drag and side force coefficients, the trajectories take on a simple parabolic form, and enables the effect of crosswinds on the trajectories to be quantified.
5. A full solution of the trajectory equations enables the trajectories to be calculated for all bowling speeds for different types of ball. Some complex trajectories, involving late swing and reverse swing, can be predicted in the Reynolds number transition region, and are most obvious where that transition is steep.

It is thus clear that the calculation method outlined above provides a useful framework for the consideration of the effects of changes in the force coefficient characteristics on the ball trajectories, and thus in principle allows the significance of the parameters that might cause such changes to be assessed. For example, one topic that is of much interest is the issue of how atmospheric conditions affect cricket ball swing. Specifically, there is much anecdotal evidence from players that cricket balls swing more in overcast, humid conditions than in bright sunny conditions and the degree of swing changes rapidly with changes in weather conditions. The trajectory calculations presented here show the importance of the force coefficient transition region. This has been appreciated qualitatively by many investigators in the past and several suggestions have been made as to how atmospheric properties affect this transition region. However, the common suggestions, that atmospheric conditions affect density and viscosity (and thus Reynolds number) or that humidity affects

the seam height and thus the boundary layer transition/separation behaviour, have been shown to be inadequate by a number of investigators (see reference [**3**] for a discussion of this). This is only reasonable, as all the parameters mentioned are bulk parameters of the atmosphere and would thus change over a timescale of an hour or more following a change in weather conditions, and would not produce the very rapid changes in ball behaviour observed by players. In the author's opinion there is only one such parameter that could produce such effects in the much shorter timescales (of the order of minutes) that are experienced by players: the solar radiation itself. It can be conjectured, very speculatively, that the effect of variable solar radiation on the ball, in causing expansion/contraction of the seam, or in causing convection currents around the surface of the ball by direct heating of the ball or through the release of latent heat in water evaporation, may disrupt the boundary layer transition/separation processes around the ball and thus modify the parameters of the force coefficient transition region. This is possibly a fruitful area for future research, in which the calculation framework outlined above could be used to assess the importance or otherwise of any effects that are observed.

Finally, it is worth mentioning that the modelling contained in this article could ultimately be part of a larger modelling exercise that would also investigate the movement of the interaction of the flight of the ball towards the batsman, with the bounce of the pitch and the subsequent secondary flight of the ball. The impact/bounce phase of this problem has recently been investigated in detail in reference [**19**], but much work remains to be done in this area.

REFERENCES

1 **Mehta, R. D.** Aerodynamics of sports balls. *Annu. Rev. Fluid Mech.*, 1985, **17**, 151–189.
2 **Mehta, R. D.** Cricket ball aerodynamics: myth versus science. In *The engineering of sport – research, development and innovation* (Eds A. J. Subic and S. J. Haake), 2000, pp. 153–167 (Blackwell Science, London).
3 **Mehta, R. D.** A review of cricket ball swing. *Sports Eng.*, 2005, **8**, 181–192.
4 **Bentley, K., Varty, P., Proudlove, M.,** and **Mehta, R. D.** An experimental study of cricket ball swing. Imperial College Aero Technical Note, 1982, pp. 82–106.
5 **Baker, C. J.** The debris flight equations. *J. Wind Eng. Ind. Aerodyn.*, 2007, **95**(5), 329–353.
6 **Quinn, A. D., Hayward, M., Baker, C. J., Schmid, F., Priest, J. A.,** and **Powrie, W.** A full-scale experimental and modelling study of ballast flight under high-speed trains. *Proc. IMechE, Part F: J. Rail and Rapid Transit*, 2010, **224**(F2), 61–74. DOI: 10.1243/09544097JRRT294.
7 **Holmes, J. D., Baker, C. J.,** and **Tamura, Y.** Tachikawa number: a proposal. *J. Wind Eng. Ind. Aerodyn.*, 2005, **94**(2006), 41–47.
8 **Alam, F., La Brooy, R., Watkins, S.,** and **Subic, A.** An experimental study of cricket ball aerodynamics. In Proceedings of the International Conference on *Mechanical engineering*, (ICME2007), Dhaka, Bangladesh, 2007.
9 **Alam, F., La Brooy, R., Subic, A.,** and **Watkins, S.** Aerodynamics of cricket balls – an effect of seams. In Proceedings of the 7th ISEA Conference 2008, Biarritz, 2–6 June 2008.
10 **Barton, N. G.** On the swing of a cricket ball in flight. *Proc. R. Soc. Lond. A*, 1982, **379**, 109–131.
11 **Hunt, C.** *The aerodynamics of a cricket ball*. BSc Dissertation, Department of Mechanical Engineering, University of Newcastle, UK, 1982.
12 **Ward, C. W.** The aerodynamics of a cricket ball. Department of Mechanical Engineering, University of Newcastle, UK, 1983.
13 **Sayers, A. T.** On the reverse swing of a cricket ball – modelling and measurements. *Proc. IMechE, Part C: J. Mechanical Engineering Science*, 2001, **215**(C1), 45–55. DOI: 10.1243/0954406011520508.
14 **Sayers, A. T.** and **Hill, A.** Aerodynamics of a cricket ball. *J. Wind Eng. Ind. Aerodyn.*, 1999, **79**, 169–182.
15 **Sherwin, K.** and **Sproston, J. L.** Aerodynamics of a cricket ball. *Int. J. Mech. Edu.*, 1982, **10**, 71–79.
16 **Brouy, L. R., Alam, F.,** and **Watmuff, J.** New methods of initiating reverse swing on a cricket ball. The Engineering of Sport III, Honolulu, Hawaii, USA, 2009.
17 **Imbrosciano, A.** *The swing of a cricket ball*. Project report, Newcastle College of Advanced Education, Newcastle, Australia, 1981.
18 **Cook, N. J.** *A designer's guide to wind loading on building structures – part 1*, 1985 (Butterworths, London).
19 **Carré M. J., James, D. M.,** and **Haake, S. J.** Impact of a non-homogeneous sphere on a rigid surface. *Proc. IMechE, Part C: J. Mechanical Engineering Science*, 2004, **218**(C3), 273–281. DOI: 10.1243/095440604322900408.

APPENDIX

Notation

A	ball cross-sectional area
C_D	drag force coefficient, $D/0.5\rho Aq^2$
C_S	side force coefficient, $S/0.5\rho Aq^2$
d	diameter of the cricket ball
D	drag force
g	acceleration due to gravity
m	mass of the ball
n	seam angle
q	bowling speed
Q	total ball velocity relative to the air $[(\bar{u}-\bar{U})^2+(\bar{v}-\bar{V})^2+(\bar{w}-\bar{W})^2]^{0.5}$
Re	Reynolds number, $q\rho d/\mu$
S	side force
t	time
$\bar{t}$	tg/q
T	Tachikawa number, $\rho Aq^2/2\,mg$

u	longitudinal ball velocity
$\bar{u}$	u/q
U	longitudinal wind speed
$\bar{U}$	U/q
v	lateral ball velocity
$\bar{v}$	v/q
V	lateral wind speed
$\bar{V}$	V/q
w	vertical ball velocity
$\bar{w}$	w/q
W	vertical wind speed
$\bar{W}$	W/q
x	longitudinal co-ordinate
$\bar{x}$	xg/q^2
y	lateral co-ordinate
$\bar{y}$	yg/q^2
z	vertical co-ordinate
$\bar{z}$	zg/q^2
α	initial inclination angle
μ	dynamic viscosity of air
ρ	density of air